Numerical Simulation of Turbulence Anisotropy with Reynolds Averaged Navier-Stokes Models

Fernando Nóbrega de Araujo, André Luiz Tenório Rezende
Department of Mechanical and Materials Engineering, IME - Military Engineering Institute, 22290-270, Rio de Janeiro, RJ, Brazil

***Abstract* — A understanding of the RANS methodology limitations is gained through a series of numerical simulations of the incompressible flow around a thin flat plate of infinite wingspan at small incidences. In this flow, a thin recirculation zone with highly anisotropic turbulent structures is formed close to the leading edge after boundary layer separation. The importance of capturing anisotropy is thoroughly examined and quantitatively accessed in this paper, through a number of simulations employing several RANS approaches with different levels of anisotropy representation, ranging from the *k-w SST* 2-equation model, to the more complex Reynolds Stress Tensor Model (RSM). The solutions are obtained through the Reynolds Averaged Navier-Stokes (RANS) equations for the two-dimensional steady state flow, and the results are compared with available wind tunnel experimental data.**

***Keywords* — anisotropy , flat plate, reattachment.**

I. INTRODUCTION

Turbulent numerical simulations with the Reynolds Averaging Navier-Stokes methodology (RANS) present three main inherent weakness. The first one relates to its steady state regime, in which every transient evolution is sumarely supressed from the simulation and left to be modeled by transport equations involving a lot of heuristic assumptions, not rarely leading to unphysical behaviors. The second weakness regards its unability to capture three dimensional vortex brakedown, whose role in turbulent evolution is well know and too important to be discarded. In fact, for a flow with a homogeneous direction in the statistical sense, like an airfoil with an infinite wingspan, even if a three dimensional mesh is employed, RANS simulations will never be able to predict different evolutions for each of the cross-sections, simply because it is a steady state methodology which only deals with statistical fields. Since this kind of flow is statistically homogeneous in one direction, say, the wingspan, every cross-section of the geometry will have the same resulting field from RANS. Therefore, with traditional assumptions that relates transport of momentum and other physical quantities to the gradient of the fields, no variable can be transported in the wingspan direction, and no vortex brakedown can be correctly captured. A third weakness inherent to many RANS models is related to the Boussinesq hypotheses, by which the Reynolds stress tensor is supposed aligned with the strain rate by means of a turbulent viscosity. In two dimensional flows, it can be mathemathically shown that this implies that, discounting the homogeneous direction elements, the remaining Reynolds stress is isotropic. This latter issue means that those RANS models based on the Boussinesq hypotheses are not expected to correctly predict situations involving flows with strong anisotropy.

The first and second of the above mentioned weakness can be only overcome if a transient formulation of the RANS equations is employed, which is known in the literature as Unsteady Reynolds Averaging Navier-Stokes methodology (URANS). Very often, however, the dissipation levels provided by the modelling are too high to allow the development of transient structures, and URANS reverts to traditional RANS converging to a steady state field solution.

The third of the above mentioned weakness is overcome by a class of models known as Reynolds Stress Models, in which, instead of the Boussinesq hypothesis, a transport equation for the Reynolds stress tensor is derived, which at least in principle allows the correct prediction of turbulent anisotropies.

The objective of this work is to isolate and understand the implications of each of these inherent limitations presented by RANS methodology. In order to do so, it was chosen the incompressible flow over a thin flat plate at small incidence as the test case, which is a very challenging scenario for turbulence modelling with its strong anisotropies. The mesh was chosen after a previous careful convergence study so that it is fine enough to resolve near wall structures, with the maximum value of y^+ equal to 1.

Two different levels of RANS modelling were tried and compared to experimental data: firstly, the simple two equation models k-ω SST, were run to understand the limitations of the most basic and traditional model; secondly, the complete RSM from (Launder, 1989) gave us an idea about what can ultimately be achieved before breaking the barrier of 2D steady-state simulations to try a more expensive transient or even 3D simulation.

II. TEST CASE – FLOW OVER A THIN FLAT PLATE

The understanding of the flow around thin flat plate at shallow incidence can help in the design of airfoils and sails (Cyr, Newman, 1996), as well as flexible wing-based micro air vehicles (Lian and Shyy, 2005). The flow around an inclined flat plate with a sharp leading edge, as shown in Fig. 1, results in a long and thin bubble, denominated “thin aerofoil bubble” (Gault, 1957). At zero incidence angle, the stream is laminar and attached on both sides, generating zero lift (assuming equal surface profiles). If the plate has an incidence angle, the stagnation point moves to the inferior surface. The boundary layer around the leading edge is very thin, and it is expected to separate immediately, due to the flow direction change. The fixed separation point leads to the hypothesis that the flow will be insensitive to a change in Reynolds number, as long as laminar to turbulent shear-layer transition occurs soon after separation. According to experimental data (Crompton, 2001) this happens for Reynolds numbers above 10^5.

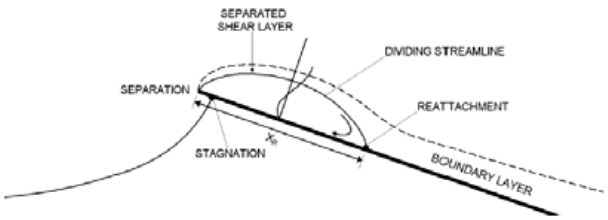

Fig. 1. Simplified model of a thin aerofoil separation bubble.

The thin aerofoil bubble created on a plate with a sharp leading edge is consequently characterized by a flow separation at the leading edge with a consequent reattachment to the upper surface at a point which moves gradually downstream with increasing incidence. If the incidence angle is sufficiently small (usually smaller than 5 degrees), the flow reattaches. As shown in Fig. 1, there is a dividing streamline which demarcates the bubble from the outer flow and which rejoins the surface at the reattachment point. For angles greater than 5 degrees, there is no reattachment point, and the bubble enlarges downstream into the wake (Newman and Tse, 1992).

Subsequent to separation, the lack of a wall viscous damping makes the shear layer suffer a quick transition to turbulent regime very close to the leading edge. The turbulent shear layer thickens rapidly and has a high entrainment rate; it then reattaches further downstream where the streamlines bifurcate. One branch goes back towards the leading edge to feed the shear layer. The resultant backflow reduces the pressure at the surface and in turn helps to bend the shear layer back to the reattachment point. If the chord is long enough to allow a reattachment, the other branch is driven downstream in the form of an attached turbulent boundary layer until it reaches the trailing edge.

From an academic point of view, this flow configuration provides an interesting and challenging test case where several aspects of turbulence modelling and numerical schemes can be examined. Because of its rich variety of important turbulent phenomena, specially its strongly anisotropic structures, several traditional turbulence modelling fail to predict even the simpler first order velocity statistics, pressure coefficients, and crytical characteristics such as the reattachment length. In some ways, it can be considered the external version of the classic backward facing step benchmark test case (Choi, Moin, 1994). In fact, both test cases present a very well-defined point of separation, determined by a sharp edge in the geometry from where a stream of vortices are shed, a principal recirculating structure, and not rarely further separations and reattachments are observed in the mean velocity field, in the form of secondary recirculation bubbles. However, the level of turbulence anisotropy that can be obtained in the flow around thin flat plate is not achievable by simple backward facing step configuration. Added to the larger computational domain, which requires several compromises in the mesh design to obtain correct representation of structures of different sizes while keeping the total computational cost feasible, this external version of the backward facing step can be considered a lot more challenging and an important tool for validate and develop better turbulence modelling approachs.

This complex flow around a plate at the shallow incidence has been experimentally investigated by Crompton (2001). Detailed velocity and turbulence statistics were measured in wind tunnel for the leading edge bubble with the use of Laser Doppler Anemometry (LDV) for inclination angles of the flat plate varying from 1 to 5 degrees with a Reynolds number chord of 2.13×10^5. Following the work of Crompton, numerical studies based on Reynolds Average Navier-Stokes methodology (RANS) with the k-ω and SST models were developed by Collie (2005). Due to the inability of Reynolds Average models (RANS) to capture the strong anisotropy of this type of flow, Sampaio et al. (2006a, 2006b) employed the Large-Eddy Simulation (LES) methodology to the same thin flat plate test case, with an incidence angle of one degree, aiming at a better understanding of the physics involved. Although, better agreement with experimental data was obtained, a need for a carefull mesh study was identified.

III. MATHEMATICAL MODEL

The Reynolds-averaged approach is based on decomposing the velocity as $\mathbf{u}=\overline{\mathbf{u}}+\mathbf{u}'$ where $\overline{\mathbf{u}}$ is the average velocity vector and $\mathbf{u}'$ the velocity vector fluctuation. The average continuity and momentum equation (RANS), for a steady state incompressible flow is given by

$$\nabla \bullet \overline{\mathbf{u}} = 0 \quad ; \tag{1}$$

$$\nabla \bullet (\overline{\mathbf{u}}\,\overline{\mathbf{u}}) = -\nabla\left(\frac{p}{\rho}\right) + \upsilon \nabla^2 \overline{\mathbf{u}} + \nabla \bullet \left(-\overline{\mathbf{u}'\,\mathbf{u}'}\right)$$

where ρ is the density, $\upsilon=\mu/\rho$ is the cinematic viscosity, μ is the molecular viscosity, and p is the pressure. Equation (1) has the same form of the Navier-Stokes equation, but now it has an additional term, the turbulent Reynolds stress term, $-\overline{\mathbf{u}'\mathbf{u}'}$, representing the influence of the fluctuation on the average flow. In order to close Eq. (1), the turbulent Reynolds stress can be modeled based on the Boussinesq hypothesis, where the turbulent stress is obtained through an analogy with Stokes law, i.e., the stress is proportional to the deformation rate. The turbulence models selected to be investigated at the present work are described next.

3.1. SST k-ω Model

The Shear-Stress Transport (SST) k-ω RANS model (Menter, 1994) was proposed for aeronautical flows simulations with strong adverse pressure gradients and separation by combining the k-ε and k-ω models. For boundary layers flows, the k-ω model is superior to the k-ε model in the solution of the viscous near-wall region, and has been applied with success in problems involving adverse pressure gradients. However, the k-ω model requires a non-zero boundary condition on ω for non-turbulent free-stream, and the calculated flow is very sensitive to the specified value (Menter, 1994). It has also been shown (Cazalbou et al , 1993) that the k-ε model does not suffer this deficiency. Therefore, the SST k-ω model blends the robust and precise formulation of the k-ω model close to walls with the

freestream independence of the k-ε model outside the boundary layer. To accomplish this, the k-ε model is written in terms of the specific dissipation rate, ω. Then, the standard k-ω model and the transformed k-ε model are both multiplied by a blending function and both models are added together. This blending function F_1 is zero (leading to the standard k-ω model) at the inner edge of a turbulent boundary layer and set to a unit value (corresponding to the standard k-ε model) at the outer edge of the layer.

The turbulent eddy viscosity is formulated as follows:

$$\upsilon_t = \frac{\kappa / \omega}{\max(1; S F_2 / (0.31\,\omega))} \quad ; \quad F_2 = \tanh\left(\Phi^2\right) \quad ; \quad \Phi = \max\left(\frac{2\sqrt{\kappa}}{0.09\,\omega\, d}; \frac{500\,\upsilon}{d^2 \omega}\right) \quad (2)$$

where $S = (2\,\overline{Sij}\,\overline{Sij})^{0.5}$ is the modulus of the mean rate-of-strain tensor $\overline{Sij}$, and F_2 is the blending function for the turbulent eddy viscosity in the SST k-ω model, d is the distance to the wall. The turbulent kinetic energy k and specific dissipation rate ω of the SST k-ω model (Menter, 1994) can be determined by the solution of its conservation equations, where the set of closure constants for the SST k-ω model ϕ are calculated using a blend between the constants ϕ_1 of the standard k-ω and and ϕ_2 of the k-ε model as: $\phi = F_1\,\phi_1 + (1 - F_1)\,\phi_2$.

3.2. Reynolds Stress Model (RSM)

Abandoning the isotropic eddy-viscosity hypothesis, the RSM closes the Reynolds-averaged Navier-Stokes equations by solving transport equations for the Reynolds stresses, together with an equation for the dissipation rate. This means that five additional transport equations are required in 2D simulation. The Reynolds stress transport equation can be derived from the Navier-Stokes equation.

$$\frac{\partial\, \overline{u_i'\, u_j'}}{\partial\, t} + \overline{u}_k \frac{\partial\, \overline{u_i'\, u_j'}}{\partial\, x_k} = \frac{\partial}{\partial\, x_k}\left[\left(\upsilon + \frac{\upsilon_t}{\sigma_\kappa}\right)\frac{\partial\, \overline{u_i'\, u_j'}}{\partial\, x_k}\right] + P_{ij} + \Psi_{ij} - \frac{2}{3}\delta_{ij}\varepsilon \quad (3)$$

where P_{ij} is the stress production, ψ_{ij} is pressure strain, which needs modeling and ε is the dissipation, obtained by the solution of its conservation equation, like the traditional κ–ε model.

$$P_{ij} = -\left(\overline{u_i'\, u_k'}\,\frac{\partial\, \overline{u}_j}{\partial\, x_k} + \overline{u_j'\, u_k'}\,\frac{\partial\, \overline{u}_i}{\partial\, x_k}\right) \quad (4)$$

IV. RESULTS

The thin flat plate proposed by Crompton (2000) was modeled with the geometry described in Fig. 2. The plate has a chord length c of 160 mm and a span of 800 mm giving an aspect ratio of 5, which is sufficient to supply nominally two-dimensional flow.

The reattachment length was found by Crompton (2000) to be independent of **Re** above 10^5, where **Re** is defined as **Re**= $U_\infty\, c\, /\upsilon$, where U_∞ is the free stream velocity, and c the chord length. The wind tunnel investigation was carried at **Re** = 2.13×10^5 and this Reynolds number is used to compare the turbulence models and the experiments. Attack angles, α = 1 to 5 degrees, are available in experimental data in 1 degree intervals. At inclination of 5 degrees the flow is separated for the majority of the length of the plate. The LDV measurements for the mean velocity and a few turbulent quantities over the plate are available at Crompton´s study (2000).

Fig. 3 shows the computational domain used in simulations, which was defined based on the work of Collie (2005). At the inlet, the cartesian components of velocity are set according to the angle of attack and the turbulence intensity of the freestream defined as

$$\zeta = \frac{1}{3}\frac{(\overline{u'u'} + \overline{v'v'} + \overline{w'w'})}{U_\infty^2} = \frac{2}{3}\frac{\kappa}{U_\infty^2} \quad (5)$$

is set as 0.05%, as measured in wind tunnel (Crompton, 2000). Constant pressure equal to the freestream p_∞ was set at the outlet.

Fig. 2. Thin flat plate dimensions.

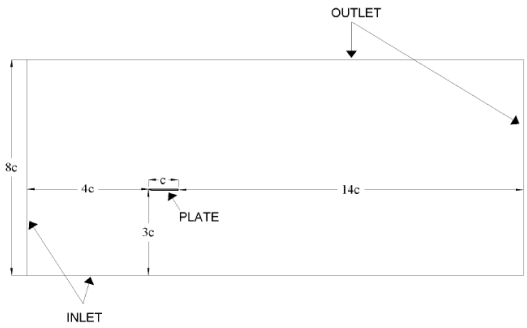

Fig. 3. Domain details.

The mesh was created with 1.5×10^5 cells, a slightly larger number of points than employed by Collie (2005), based on a grid convergence study performed by him. The distance of first node above the plate was designed as 6.25×10^{-5} c (c is the length of the chord) to guarantee $y^+ = (\tau_s/\rho)^{0.5}\, y/\upsilon$ around 1, which is the value indicated for both RANS, where τ_s is the wall shear stress.

The flow field was determined with the commercial software Fluent (2006) for models SST κ–ω and RSM .This code is based in Finite Volume Method. The QUICK scheme (Leonard, 1979) was employed in all cases to discretize the governing equations. The pressure-velocity coupling was handled by the SIMPLE algorithm. The system of algebraic equation was solved with the Multgrid method (Hutchinson and Raithby, 1986). The problem was considered converged when the maximum residue of all equations was smaller than 10^{-6}.

4.1. Reattachment Length

Table 1 presents the reattachment lengths (X_R) for the flat plate at 2 º incidence angle, obtained by turbulence models.

TABLE 1 – NORMALIZED REATTACHMENT LENGTHS (X_R) AND RESPECTIVE ERRORS.

	Experimental Crompton (2000)	SST	RSM
X_R / c	0.275	0.295	0.303
Error	-	7.3%	10.2%

The prediction accuracy of the reattachment lengths for this flow is strongly dependent on the ability of the turbulence model to represent the complex flow structure described; however the mesh refinement also plays a crucial part on this performance.

4.2. Mean Velocities Profiles

The mean velocities profiles obtained with SST and RSM models for the incidence angle $\theta = 2^{o}$ are compared with the experimental data of Crompton (2000) at two stations in Fig. 4. Both stations are located inside the bubble.

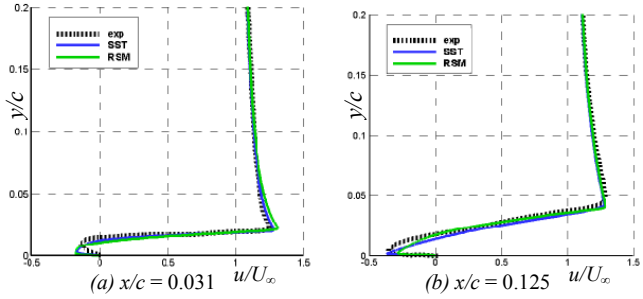

(a) $x/c = 0.031$ (b) $x/c = 0.125$

Fig. 4. Velocities profiles for incidence angle $\theta = 2^{o}$.

The velocity profiles, in the two initial stations (x/c = 0.031 ; 0.125) of Fig. 4, which are inside the bubble, show that the experimental data has a more laminar profile in comparison with the RANS turbulence models results which all experience a sharp increase in velocity over the near-wall region. To simulate the process of relaminarization an appropriate transition model is required which is not provided by the RANS models investigated, consequently these models predict greater velocity gradient in this wall region.

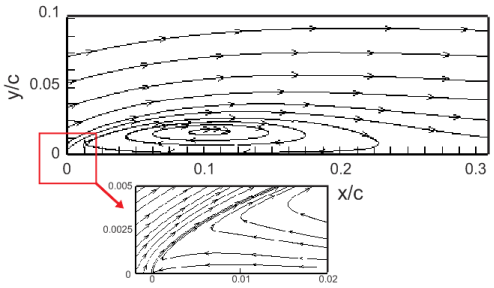

Fig. 5. Streamlines for SST model - $\theta = 2^{o}$.

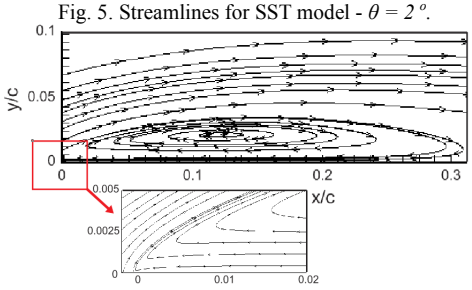

Fig. 6. Streamlines for RSM model - $\theta = 2^{o}$.

Figs.5 and 6 shows the streamlines corresponding to the predictions of SST and RSM models. It can be verified that both models were not able to predict the second recirculation bubble, which is observed experimentally.

4.3. Pressure Distributions

The pressure distribution is analyzed through the pressure coefficient defined as

$$C_P = (p_\infty - p) / (0.5\ \rho\ U_\infty^2) \qquad (6)$$

where p is the static pressure, p_∞ and U_∞ are the freestream pressure and velocity. Fig.7 presents the variation of the pressure coefficient along the plate for θ =2°. Again the RANS models SST and RSM are compared with the experimental data. These results confirm the discussion of the previous section, i.e., the turbulence models overpredict the velocity magnitude near the wall, therefore, as expected the pressure distribution is underpredict.

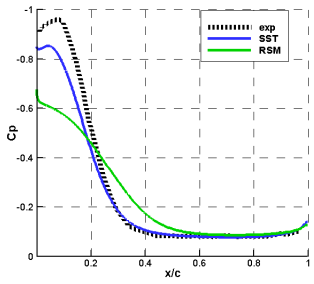

Fig. 7. Pressure coefficient for angle of attack $\theta = 2^{o}$.

4.4. Second Order Statistics

Turbulence is known to exert significant influence over development of downstream flow, most notably when separation is imminent. Although it is not the case in this particular study because the plate is flat, in future simulations one may be interested in simulating curved airfoils which may be prone to stall. In that case, the correct prediction of turbulent fluctuations is of paramount importance and for this reason we also present the main results for the component $\overline{u'u'}$.

Fig. 8 presents the component $\overline{u'u'}$ for the same two stations located above the plate. It is clear that both SST and RSM were satisfactorily accurate, and it can be said that the general behavior, magnitude of the peaks and other aspects were reasonably well predicted.

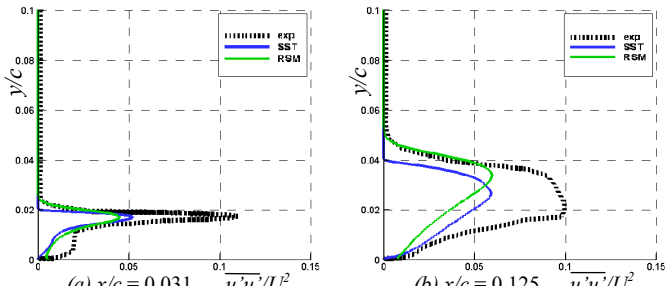

(a) $x/c = 0.031$ $\overline{u'u'}/U_\infty^2$ (b) $x/c = 0.125$ $\overline{u'u'}/U_\infty^2$

Fig. 8. Second order statistics for angle of attack $\theta = 2^{o}$.

Figs. 9, 10, 11 and 12 shows the contours for the components $\overline{u'u'}$ and $\overline{v'v'}$ of the Reynolds tensor. It can be verified on contours below, that SST model is more isotropic, compared to the normal stresses, than the RSM model. As noted previously, the SST model predicts lower values for the normal stresses.

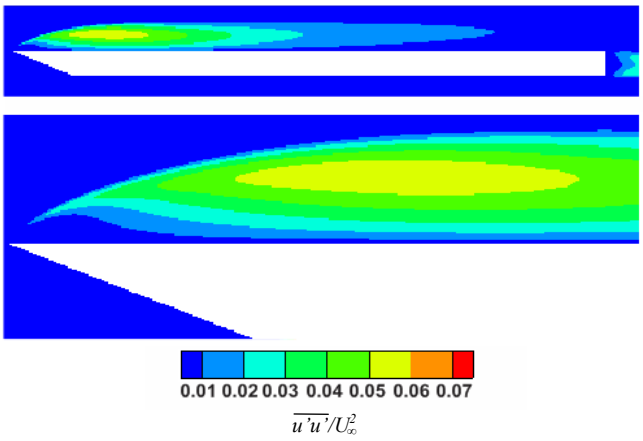

Fig. 9. Contours for the component $\overline{u'u'}$ of the Reynolds tensor (SST model - $\theta = 2^o$)

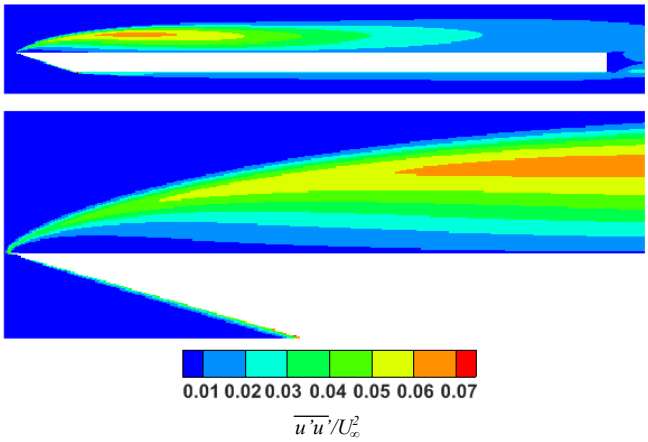

Fig. 10. Contours for the component $\overline{u'u'}$ of the Reynolds tensor (RSM model - $\theta = 2^o$)

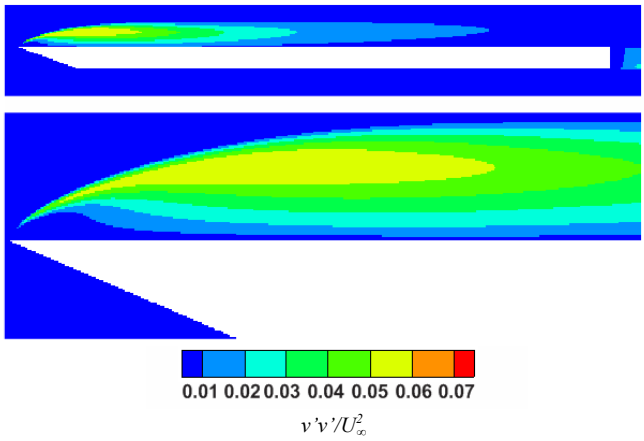

Fig. 11. Contours for the component $\overline{v'v'}$ of the Reynolds tensor (SST model - $\theta = 2^o$)

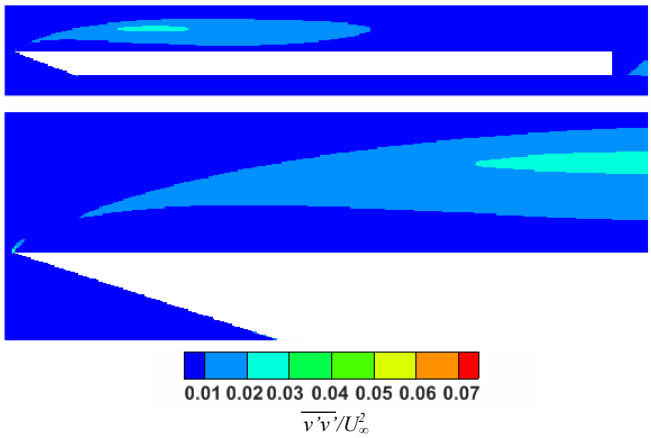

Fig. 12. Contours for the component $\overline{v'v'}$ of the Reynolds tensor (RSM model - $\theta = 2^o$)

V. CONCLUSION

In the present work, the turbulence models of SST (Menter, 1994) and RSM (Launder, 1989) were applied to determine the incompressible flow over a flat plate with a sharp leading edge, with small inclination angles, and the results were compared with experimental data of Crompton (2000).

The mean velocities profiles presented reasonable agreement with the experimental results; however the details of the recirculating bubble were underpredicted in size and overpredicted in magnitude.

No RANS model showed a clear advantage over the others, the only exception being the RSM, for the specific case of second order turbulence, where the model gave better results. This is by no coincidence, as the original idea was to try to predict and follow the evolutions of the tensor. That said, it is not clear that the additional costs involved in the RSM simulations, not to mention the difficulties to get a converged solution, did pay off in the end. In fact, the quality of the predictions of second order statistics did not translate directly towards improvements of quantities of practical engineering interest, like first order statistics, reattachment length, Strouhal number, etc.

Overall, among RANS models and considering cost-accuracy compromises, results from the SST were better. No significant and clear advantage is brought by the use of more expensive models, unless one is really interested in second order statistics.

The difficulty to capture the entrainment of the separated shear layer, encourage the investigation of the problem with more demanding models such as LES and DNS.

ACKNOWLEDGEMENTS

The authors acknowledge the support awarded to this research by the Brazilian Research Coordinate, CAPES.

REFERENCES

[1] Cazalbou, J.B., Spalart, P.R., Bradshaw, P., 1993, "On the Behavior of 2-Equation Models at the Edge of a Turbulent Region", Physics of Fluids, Vol. 6, No. 5, pp. 1797-1804.

[2] Choi, H., and Moin, P., 1994, Effects of the computational time step on numerical solutions of turbulent flow, Journal of Computational Physics, Vol. 113, pp. 1-4;

[3] Collie, S., 2005, "Application of CFD to Two-Dimensional Downwind Sail Flows", PhD Thesis, Department of Mechanical Engineering Science of the University of Auckland, New Zealand.

[4] Crompton, M. J.; Barret, R. V., 2000, "Investigation of the Separation Bubble Formed Behind the Sharp Leading Edge of a Flat Plate at Incidence". Proceedings of the Institution of Mechanical Engineers Part G-Journal of Aerospace Engineering, Vol. 214, No. G3, pp. 157-176.

[5] Crompton, M., 2001, "The Thin Airfoil Leading Edge Separation Bubble", PhD Thesis, Department of Aerospace Engineering University of Bristol.

[6] Cyr S, Newman BG, 1996, "Flow past two-dimensional membrane aerofoils with rear separation", Journal Of Wind Engineering And Industrial Aerodynamics, Vol. 63 (1-3): Pp.1-16.

[7] Durbin, P. A., 1991, ''Near-Wall Turbulence Closure Without Damping Functions,'' Theoretical and Computational Fluid Dynamics,Vol. 3, No.1, pp. 1–13.

[8] Fluent User's Guide, v. 6.2, 2006, Fluent Inc., New Hampshire.

[9] Gault, D. E., 1957, An investigation at low speed of the flow over a simulated flat plate at small angles of attack using pitot static and hot-wire probes, Technical Report TN-3876, NACA.

[10] Hutchinson, B. R., and Raithby, G.D., 1986, "A Multigrid Method Based on the Additive Correction Strategy", Numerical Heat Transfer, vol. 9, pp.511-537.

[11] Launder, B.E., 1989, "Second-Moment Closure: Present and Future?", International Journal Heat Fluid Flow, Vol. 10, No. 4, pp. 282-300.

[12] Leonard, B.P. 1979, "A Stable Accurate Convective Modeling Procedure Based on Quadratic Upstream Interpolation", Computer Methods in Applied. Mechanics and Engineering, Vol.19, pp. 59-88.

[13] Lian YS, Shyy W, 2005, "Numerical simulations of membrane wing aerodynamics for micro air vehicle applications", Journal Of Aircraft Vol. 42 (4): pp. 865-873.

[14] Menter, F. R., 1992, "Influence of Freestream Values on k-ω Turbulence Model Predictions", AIAA Journal, Vol. 30, No. 6, pp. 1657-1659.

[15] Menter, F. R., 1994, "Two-Equation Eddy-Viscosity Turbulence Models for Engineering Applications", AIAA Jounal, Vol. 32, No. 8, pp. 1598-1605.

[16] Menter, F. R., Kuntz, M., Langtry, R., 2003, "Ten Years of Industrial Experience with the SST Turbulence Model", Proceedings of the 4th International Symposium on Turbulence, Heat and Mass Transfer, pp. 625-632.

[17] Newman B.g., Tse M.c., 1992, "Incompressible Flow Past a Flat Plate Aerofoil With Leading Edge Separation Bubble", Aeronautical Journal Vol. 96, No. 952, pp. 57-64.

[18] Launder, B.E., 1989, "Second Moment Closure: Present... and Future?", *Inter. J. Heat Fluid Flow* Vol. 10, No. 4, pp. 282-300.

[19] Sampaio, L.E.B., Nieckele, A. O., Gerritsen, M. and Collie, S., 2006a, "Numerical Simulations Of The Long Recirculation Bubbles Formed In Incompressible Aerodynamic Flows Over Thin Flat Plates At Shallow Incidence", Proceedings of the 11th Brazilian Congress of Thermal Sciences and Engineering -- ENCIT 2006, Paper CIT06-0278

[20] Sampaio, L.E.B., Nieckele, A. O., Gerritsen, M. and Collie, S., 2006b, "Large Eddy Simulations of the Long Recirculation Bubbles Formed in Thin Flat Plates at Shallow Incidence", Proceedings of the 5th Spring School of Transition and Turbulence, EPTT2006, Paper ETT06-15.